Hamid Baniasadi[1]
G. A. Nagana Gowda[2]
Haiwei Gu[2]
Ao Zeng[1]
Shui Zhuang[1]
Nicholas Skill[3]
Mary Maluccio[3*]
Daniel Raftery[1,2,4]

[1]Department of Chemistry,
 Purdue University, West
 Lafayette, IN, USA
[2]Mitochondria and Metabolism
 Center, Department of
 Anesthesiology and Pain
 Medicine, University of
 Washington, Seattle, WA, USA
[3]Department of Surgery, Indiana
 University, Indianapolis, IN,
 USA
[4]Fred Hutchinson Cancer
 Research Center, Seattle, WA,
 USA

Research Article

Targeted metabolic profiling of hepatocellular carcinoma and hepatitis C using LC-MS/MS

Hepatitis C virus (HCV) infection of the liver is a global health problem and a major risk factor for the development of hepatocellular carcinoma (HCC). Sensitive methods are needed for the improved and earlier detection of HCC, which would provide better therapy options. Metabolic profiling of the high-risk population (HCV patients) and those with HCC provides insights into the process of liver carcinogenesis and possible biomarkers for earlier cancer detection. Seventy-three blood metabolites were quantitatively profiled in HCC ($n = 30$) and cirrhotic HCV ($n = 22$) patients using a targeted approach based on LC-MS/MS. Sixteen of 73 targeted metabolites differed significantly ($p < 0.05$) and their levels varied up to a factor of 3.3 between HCC and HCV. Four of these 16 metabolites (methionine, 5-hydroxymethyl-2′-deoxyuridine, *N*2,*N*2-dimethylguanosine, and uric acid) that showed the lowest *p* values were used to develop and internally validate a classification model using partial least squares discriminant analysis. The model exhibited high classification accuracy for distinguishing the two groups with sensitivity, specificity, and area under the receiver operating characteristic curve of 97%, 95%, and 0.98, respectively. A number of perturbed metabolic pathways, including amino acid, purine, and nucleotide metabolism, were identified based on the 16 biomarker candidates. These results provide a promising methodology to distinguish cirrhotic HCV patients, who are at high risk to develop HCC, from those who have already progressed to HCC. The results also provide insights into the altered metabolism between HCC and HCV.

Additional supporting information may be found in the online version of this article at the publisher's web-site

1 Introduction

Hepatitis C virus (HCV) infection is a global health problem that causes significant morbidity and mortality. Worldwide, 150–170 million people are currently infected with HCV, with 3–4 million new cases and more than 350 000 deaths reported each year according to estimates from the World Health Organization (www.who.int/mediacentre/factsheets/fs164/en/)

Correspondence: Dr. Daniel Raftery, Mitochondria and Metabolism Center, Department of Anesthesiology and Pain Medicine, University of Washington, Seattle, WA 98109, USA
E-mail: draftery@uw.edu

Abbreviations: AUROC, area under the receiver-operating characteristic; **CV**, cross-validation; **HCC**, hepatocellular carcinoma; **HCV**, hepatitis C virus; **MRM**, Multiple reaction monitoring; **PLS-DA**, partial least squares discriminant analysis; **ROC**, receiver operating characteristic; **VIP**, variable importance in projection

[1]. HCV infection of the liver is a potent risk factor for the development of hepatocellular carcinoma (HCC) and HCC is associated with a high mortality and morbidity [2–4]. In addition, HCV infection alone is a risk factor for progression of HCC by a factor of more than 25 [5], and it accounts for nearly 25% of the prevalence of HCC patients [6]. Studies have shown that the prevalence of HCV in industrialized nations, such as the United States, has more than tripled since 1975 [7, 8]. As such, the incidence of HCC has risen over the ensuing years and continues to rise to a greater extent than any other cancer subtype [9]. In the United States, HCC is often diagnosed at advanced stages mainly due to the lack of simple and sensitive methods for its early detection. The near causal link between chronic viral infection and cancer

*Additional corresponding author: Dr. Mary Maluccio,
 E-mail: mmaluccio@iupui.edu

Colour Online: See the article online to view Figs. 2 and 3 in colour.

identifies a patient population whereby biomarkers of cancer risk would be instrumental in improving our current diagnostic and treatment paradigms. Better methods to identify the subset of HCV patients at highest cancer risk would allow for: (i) the establishment of more intense surveillance mechanisms, (ii) the development of chemoprevention protocols, and (iii) improved leverage for these patients with respect to liver transplant.

Metabolomics, in which a large number of small molecule metabolites are detected quantitatively, often in easily accessible biofluids, such as blood and urine, promises useful information regarding early biomarkers and altered metabolic pathways. As metabolites are the downstream products of genes and gene expression, they integrate many of the alterations caused by disease or other biological stresses. Metabolites are exquisitely sensitive to different biological states and therefore represent a promising approach to identify potential biomarkers [10–12]. Several analytical techniques, such as NMR, LC-MS, and GC-MS, have been used to detect metabolic changes in a number of cancers including liver cancer [13]. Several studies using a variety of analytical techniques have reported discovery of potential biomarkers in biological samples, such as serum, plasma, and urine, of subjects with HCC relative to healthy controls. While a few of these studies have used animal models [14–16], the majority of studies were focused on humans [3, 4, 10, 15, 17–25] using NMR [4, 10], LC-MS [3, 17, 19, 20, 25, 26], GC-MS [3, 21, 22, 24, 26], or HPLC [23] methods. These studies have reported alterations in numerous metabolic pathways, including glycolysis, amino acid, fatty acid, and bile acid metabolism based on altered metabolites in HCC. However, none of the studies have focused exclusively on altered metabolic pathways between HCV patients, and in particular those with cirrhosis, who have high risk of developing HCC, and those who have developed HCC. We recently reported that three metabolites, choline, valine, and creatinine, differentiate HCC patients from HCV using high-resolution NMR spectroscopy, and showed the potential utility of identification of such altered metabolites for identifying HCV patients with risk of developing HCC [27].

In the present work, we focus on identifying additional metabolic changes and altered metabolic pathways between HCC patients with underlying HCV and HCV patients who are at high risk of developing HCC. All patients in the study had cirrhotic livers. To extend the coverage of low concentration metabolites that distinguish HCV and HCC, we have chosen a targeted method based on LC-MS/MS metabolite profiling of serum. This multiplexed targeted LC-MS/MS approach has been shown to be quite robust and versatile in a variety of biomarker and systems biology studies [28–31]. In the present work, a number of significant changes were observed in several important and cancer-related metabolic pathways. Utilizing multivariate statistical analysis, we could combine the top performing metabolite biomarkers into a model that distinguishes between the two patient groups with excellent performance. Monitoring metabolites in HCV patients may provide improved understanding of the timing and pathogenesis of HCC, and when further developed allow identification of HCV patients who are at high risk of liver cancer at an earlier stage.

2 Materials and methods

2.1 Chemicals and reagents

Methanol was obtained from Avantor Performance Materials (HPLC-grade; Center Valley, PA, USA). Acetic acid (≥99.7%) and all the standard metabolites (≥97%) used in this study (see Supporting Information Table 1) were purchased from Sigma-Aldrich (St. Louis, MO, USA). L-Proline-$^{13}C_5$, $^{15}N_1$ (97–99 atom% ^{13}C, 97–99 atom%, ^{15}N) was purchased from Cambridge Isotope Laboratories (Andover, MA, USA). Water was purified using an EASYpure II UV water purification system (Barnstead International, Dubuque, IA, USA).

2.2 Patients and serum sample

Patient serum samples were collected from the Indiana University/Lilly Tissue Bank through clinical collaboration following protocols approved by the institutional review boards of both Indiana and Purdue Universities. Sample cohorts consisted of histologically proven HCC patients with underlying HCV and cirrhosis ($n = 30$; mean age 56 ± 10) and HCV patients with cirrhosis but without HCC ($n = 22$; mean age 52 ± 7). Table 1 shows demographic characteristics of the patient cohorts. Overnight fasted samples were collected to minimize confounding factors arising from diet. The blood samples were allowed to clot for 45 min; centrifuged at 2000 rpm for 10 min and the resulting sera were separated and aliquoted into separate tubes and frozen immediately at −70°C. The frozen samples were then shipped over dry ice to Purdue University (West Lafayette, IN, USA), which were stored at −80°C until used for analysis.

2.3 Sample preparation and acquisition

Frozen patient sera were thawed at room temperature for 30 min. Proteins were precipitated by adding 600 μL methanol to 200 μL to each serum sample. The solution was

Table 1. Demographic and clinical characteristics of the patients

Patients characteristics	HCC	HCV
Number of patients	30	22
Age (mean ± SD)	56 ± 10	52 ± 7
Gender (F/M)	0.3	0.46
Caucasian	21	20
African American	1	2
Hispanic	3	0
Unknown race/ethnicity	4	0
Middle Eastern	1	0

vortexed vigorously for 1 min and then held for 20 min at −20°C. The samples were centrifuged at 14 000 rpm for 20 min (Eppendorf centrifuge, model 5804, Hauppauge, NY, USA), and the supernatant was collected and dried using a vacuum system (Vacufuge Plus, Eppendorf). Each dried sample was reconstituted in 50 μL water/methanol (95:5) and then transferred to an LC sample vial. Labeled sample vials were placed in the autosampler in random order and kept at 4°C throughout the analysis. A 10 μL sample injection was used for LC-MS/MS analysis in both positive and negative modes. $^{13}C_5$–^{15}N-proline was added to each serum sample, after deproteinization, and used as an internal reference. Further, to assess performance of the instrument and process reproducibility, a mixture of all the metabolites was used as a quality control sample and injected into the LC-MS/MS after every 25 patient samples, as well as before and after cleaning the ESI source; the ESI source was cleaned every 48 h. Duplicate sample runs were performed to account for technical reproducibility. To evaluate sensitivity and linear dynamic ranges, we determined LODs and dynamic ranges from a mixture of 39 standard metabolites at 20 different concentrations (Supporting Information Table 2).

2.4 LC-MS/MS system components and MS parameters

Mass spectrometric analyses were performed on an AB SCIEX-3000 triple quadrupole mass spectrometer (AB SCIEX, Framingham, MA, USA) equipped with an ESI turbo ion spray source operated in both positive and negative ion modes. The mass spectrometer was coupled to an Agilent 1100 series HPLC system (Agilent Technologies, Santa Clara, CA, USA) consisting of two quaternary pumps, solvent degassers, and a temperature-controlled column oven [31]. A CTC PAL autosampler (LEAP Technologies, Carrboro, NC, USA) equipped with multiple injection ports was used for sample loading, while a VICI 2-position switching valve (Valco Instruments, Houston, TX, USA) allowed the MS inlet to be switched between the two pumps, one of which was used for separating metabolites detected as positive ions and the other as negative ions. The two pumps allowed for alternating separation and column reconditioning to increase throughput. Multiple reaction-monitoring (MRM) mode was used to detect the multiple metabolites as they eluted off of the chromatographic column using a dwell time of 100 ms per metabolite. Nitrogen gas was used as curtain, collision, and nebulizer gas, with flow rates set at 12, 10, 12 (arbitrary units), respectively. The ion spray needle voltages used for MRM positive and negative modes were set at 3600 and −3600 V, respectively. The LC-MS/MS system was controlled by Analyst 1.5 software (AB SCIEX).

2.5 Chromatography conditions

Chromatography was performed under reverse phase conditions using an Eclipse XDB-C_{18} 4.6 × 150, 5 μm column (Agilent Technologies). The flow rate, column temperature, and sample injection volume were set to 400 μL/min, 45°C, and 10 μL, respectively. The optimized chromatography conditions were as follows: Solvent A: water with 0.1% acetic acid; Solvent B: methanol with 0.1% acetic acid. The elution gradient, 0 min: 5% B; 42 min: 95% B, was used to separate metabolites detected in negative MRM mode. For positive MRM mode, 0 min: 5% B; 35 min: 95% B were used. Before all injections, column cleaning and equilibration steps were applied.

2.6 Compound optimization parameters

Information about each precursor ion m/z values (Q_1) and product ion m/z values (Q_3) for MRM detection of the metabolites was obtained from previous studies [28–31]. To decrease the chemical background noise and increase the intensity of metabolite peaks, precollision cell voltages including declustering potential (DP), focusing potential (FP), collision energy, and collision cell exit potential (CXP) parameters for each metabolite were optimized. To this end, a 2 μM solution for each metabolite in 50:50 water/methanol was prepared and was directly infused into the mass spectrometer using a Harvard PHD 2000 Syringe Pump (Holliston, MA, USA) at a flow rate of 15 μL/min. The optimized metabolite parameters were obtained and used for the appropriate MRM mode.

2.7 Data analysis

Peak intensities for the 73 measured metabolites were integrated using Analyst 1.5 software (AB SCIEX). Peak integrals for each metabolite averaged over duplicate sample runs were used for further analysis. The Student's *t*-test was used to evaluate statistical significance for metabolite intensity differences between HCC and HCV. Four metabolites that showed the lowest *p*-values between the two patient groups were then chosen for multivariate statistical analysis using partial least squares discriminant analysis (PLS-DA). PLS-DA modeling was performed using Matlab (R2008a, Mathworks, Natick, MA, USA) installed with the PLS toolbox (v4.1, Eigenvector Research, Wenatchee, WA, USA). The X matrix, consisting of the MS data, was mean centered prior to all statistical analyses. Each subject was assigned either a "0" (for HCC) or "1" (for HCV) to serve as inputs to the Y matrix. Leave-one-out cross-validation (CV) was chosen, and the number of latent variables (three in this case) was selected according to the minimum root mean square error of CV procedure. Class predictions were made visually using a Y-predicted scatter plot with a cutoff value chosen to minimize errors in class membership. The R statistical package (version 2.8.0) was used to generate receiver operator characteristic curves and box-and-whisker plots, calculate sensitivity, specificity, and area under the receiver-operating characteristic curve (AUROC). A schematic diagram of altered metabolic pathways was drawn based on established databases

(www.genome.jp; http://modomics.genesilico.pl/pathways/) to help understand the pathogenesis of the disease and indicate the relationship among the candidate biomarkers. A second multivariate PLS-DA model was constructed to analyze the sample data by selecting four metabolites based on their variable importance in projection (VIP) scores derived using all 73 metabolites, and a comparison with the results obtained using four lowest *p*-value metabolites was made.

3 Results

Targeted analysis using LC-MS/MS in MRM mode was performed on 73 metabolites that could be detected reliably in serum. Of these, 38 metabolites were detected in negative ion mode and 35 metabolites in positive ion mode (see Supporting Information Table 1 for metabolite list). All 73 metabolites were detected in all HCC and HCV patient samples and could be measured quantitatively and reliably based on the achieved MS sensitivity and chromatographic conditions (Supporting Information Fig. 1 and Table 2). Good instrumental stability was observed, indicated by the CV values of 13–20% for the metabolites in the quality control samples, based on 24 measurements, 12 in positive and 12 in negative ion mode.

Initial data analysis based on the averaged peak areas of duplicate sample runs indicated 16 metabolites (tyrosine, phenylalanine, glycerol, 1-methylguanosine, methionine, *N*-carbamoyl-β alanine, xanthine, homocysteine, creatine, 1-methyladenosine, *N*2,*N*2-dimethylguanosine, 5-hydroxymethyl-2'-deoxyuridine, 2-deoxyguanosine, 1-methylinosine, aconitic acid, and uric acid) had statistically significant differences in the samples of HCC and HCV patients, as indicated by $p < 0.05$ using the Student's *t*-test. These metabolites varied in their levels by a factor of up to 2.1 between HCC and HCV, and all except three, creatine, 1-methyladenosine, and 5-hydroxymethyl-2'-deoxyuridine were downregulated in HCC compared to HCV. Table 2 shows the 16 metabolites along with their *p*-values and fold changes between the two groups.

From the 16 distinguishing metabolites, a smaller group of metabolites was chosen, based on their low *p*-values, to build a model and test classification accuracy and predictive power. A group of four metabolites (methionine, 5-hydroxymethyl-2β'-deoxyuridine, *N*2,*N*2-dimethylguanosine and uric acid) with the lowest *p*-values ($p \leq 0.0069$) provided high classification accuracy. Box-and-whisker plots for these four potential biomarkers are shown in Fig. 1 and indicate the individual discrimination power between HCC and HCV. The median level for 5-hydroxymethyl-2'-deoxyuridine increased in HCC by factor of 1.5, while the levels for the other three metabolites decreased. A PLS-DA model combining these four metabolites was performed using leave-one-out cross validation. The model showed an excellent separation between HCC and HCV patients with a sensitivity of 97% and specificity of 95%. The receiver operating characteristic curve shown in Fig. 2 for the prediction model has an

Table 2. List of metabolites with significant mean changes between HCC and HCV patients

Metabolite	FC[a]	*p*-Value
Aconitic acid	0.7	0.029
Creatine	2.1	0.029
2-Deoxyguanosine	0.3	0.015
Glycerol	0.8	0.018
Homocysteine	0.8	0.036
5-Hydroxymethyl-2'-deoxyuridine	1.5	0.00088
Methionine	0.7	0.0032
1-Methyladenosine	1.4	0.011
1-Methylguanosine	0.6	0.0078
1-Methylinosine	0.5	0.0075
*N*2,*N*2-Dimethylguanosine	0.5	0.0018
N-Carbamoyl-β-alanine	0.7	0.016
Phenylalanine	0.9	0.013
Tyrosine	0.8	0.016
Uric acid	0.7	0.0069
Xanthine	0.8	0.011

a) FC: mean fold change (HCC/HCV).

AUROC of 0.98. R^2 and Q^2 values for the model were 0.62 each, indicating that the model had good predictability.

A second approach for metabolite selection was used based on high VIP scores. VIP analysis of the results of PLS-DA modeling using all 73 metabolites provided a number of metabolites with scores above 1. Four metabolites (5-hydroxymethyl-2'-deoxyuridine, 1-methyladenosine, 2-deoxyguanosine, and 4-hydroxybenzoic acid) were found to have the highest VIP scores. While one of the metabolites (5-hydroxymethyl-2'-deoxyuridine) thus selected was the same, three metabolites (1-methyladenosine, 2-deoxyguanosine, and 4-hydroxybenzoic acid) were different from those selected based on lowest *p*-values. The PLS-DA model developed using these four metabolites thus selected provided somewhat poorer results compared to results derived using the four metabolites with lowest *p*-values, with a sensitivity of 90% and specificity of 83%. The AUROC was also lower (0.91 vs. 0.98) (Supporting Information Fig. 2). R^2 and Q^2 analysis showed that this model was not very predictive with values of 0.04 and −0.11, respectively. Further, while three of the metabolites (5-hydroxymethyl-2'-deoxyuridine, 1-methyladenosine, and 2-deoxyguanosine) differed significantly between PC and controls ($p < 0.05$), one metabolite (4-hydroxybenzoic acid) did not differ significantly ($p > 0.05$).

Overall, the 16 distinguishing metabolites are associated with a number of important pathways (vida infra), many of which have been previously shown to be associated with cancer [3, 4, 10, 19, 21–24]. A metabolic pathway diagram was constructed highlighting the biomarker candidates and their relationship to various pathways and is shown in Fig. 3.

4 Discussion

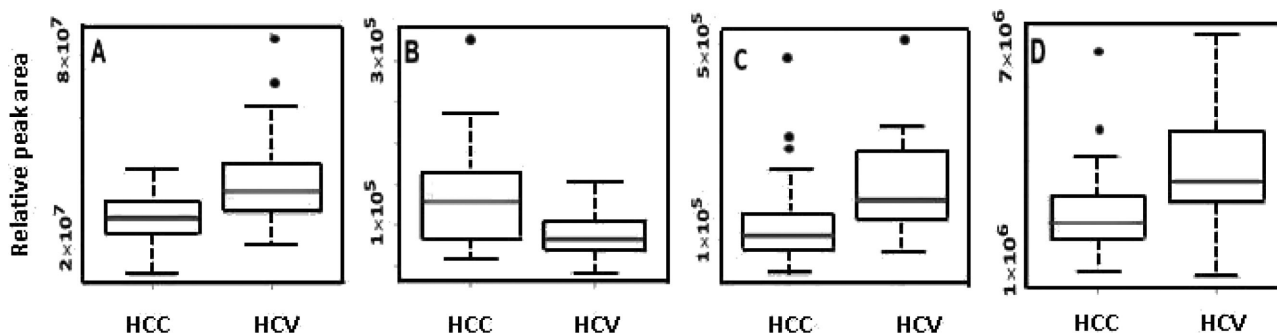Optimized chromatographic conditions and MS/MS by MRM in positive and negative ion modes enabled access to a high

Figure 1. Box-and-whisker plots for the four biomarker candidates with lowest *p* values between HCC and HCV: (A) methionine, (B) 5-hydroxymethyl-2′-deoxyuridine, (C) *N*2,*N*2-dimethylguanosine, and (D) uric acid. The middle horizontal line in a box represents the median, the bottom and top boundaries represent the 25th and 75th percentiles, respectively. The lower and upper whiskers represent the 5th and 95th percentiles, respectively, and the circles represent outliers.
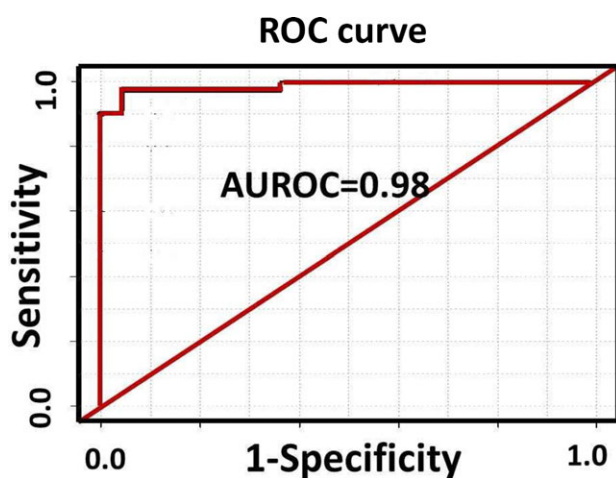

Figure 2. Receiver operating characteristic curve generated from the PLS-DA model of the four metabolites shown in Fig. 1.

number of reliably measured and important metabolites. In this study, we could detect concentrations for 73 serum metabolites in HCV patients and HCC patients with underlying HCV. These targeted metabolites span a broad range of compound classes, including amino acids (36% of total measured); organic acids (30%); nucleosides and nucleotides (12%); purines and their derivatives (7%); amino ketones (4%); and others (11%) as shown in Table 3. Sixteen of these metabolites that differed, significantly, indicate pathological differences between the two groups of patients. Further, the high sensitivity and specificity exhibited by the multivariate statistical model that distinguishes HCC and HCV is promising for better understanding the pathogenesis as well as for earlier detection of HCC in HCV infected patients (Fig. 2).

Considering that HCV is a major cause for primary liver cancer (HCC), as well as the fact that symptoms for HCC do not appear typically until the last stage of the disease, it is of significant interest to identify HCV patients with risk of developing HCC based on the identification of altered metabolites and metabolic pathways. Along these lines, we recently demonstrated the potential benefit of identifying metabolite markers in serum using NMR spectroscopy [27]. However, due to the limited sensitivity of NMR, a relatively small number of distinguishing metabolites were identified from the study. The high sensitivity of the LC-MS/MS approach used in the present study provided a much wider pool of distinguishing metabolites that are complementary to those identified by NMR. To understand the pathogenesis of the disease and indicate the relationship among candidate biomarkers, a schematic pathway diagram highlighting potential biomarker candidates and their pathway relationships is shown in Fig. 3. In the figure, metabolites that showed statistically significant alterations in intensity are shown in square boxes. The three upregulated metabolites are shown with an upward pointing arrow.

A number of altered metabolic pathways including the β-alanine pathway (metabolite: *N*-carbamoyl-β-alanine), glycolipid (glycerol), amino acid (phenylalanine, tyrosine, creatine, cysteine, methionine, homocysteine), purine (xanthine and uric acid), and nucleoside pathways (1-methyladenosine, 1-methylinosine, deoxyguanosine, 1-methylguanosine, and *N*2,*N*2-dimethylguanosine) were identified as being affected due to HCC, based on the 16 metabolites with altered levels. To the best of our knowledge, 4 of these 16 metabolites (*N*-carbamoyl-β-alanine, 5-hydroxymethyl-2′-deoxyuridine, 2-deoxyguanosine, and aconitic acid) have not been previously reported as being associated with the development of liver cancer, while 12 of 16 have been reported as potential biomarkers for liver cancer and hepatitis [3, 4, 10, 19, 21–24].

As shown in Table 2, the mean levels for all of the amino acid biomarker candidates with low *p*-values, including tyrosine, phenylalanine, methionine, homocysteine, and *N*-carbamoyl-β-alanine, decrease in HCC compared with HCV. The results are in agreement with the previous studies that reported a decrease of amino acids in malignant tumors is related to an increase demand for amino acid in the presence of tumors [32, 33]. Creatine was observed to increase in the HCC patients in agreement with previous studies that showed an increase in concentration of creatine reported in HCC and lung tissue that reflect alterations in energy metabolism [4, 34, 35]. A decrease in methionine levels may be related to the low level of serine in the serum of HCC patients that
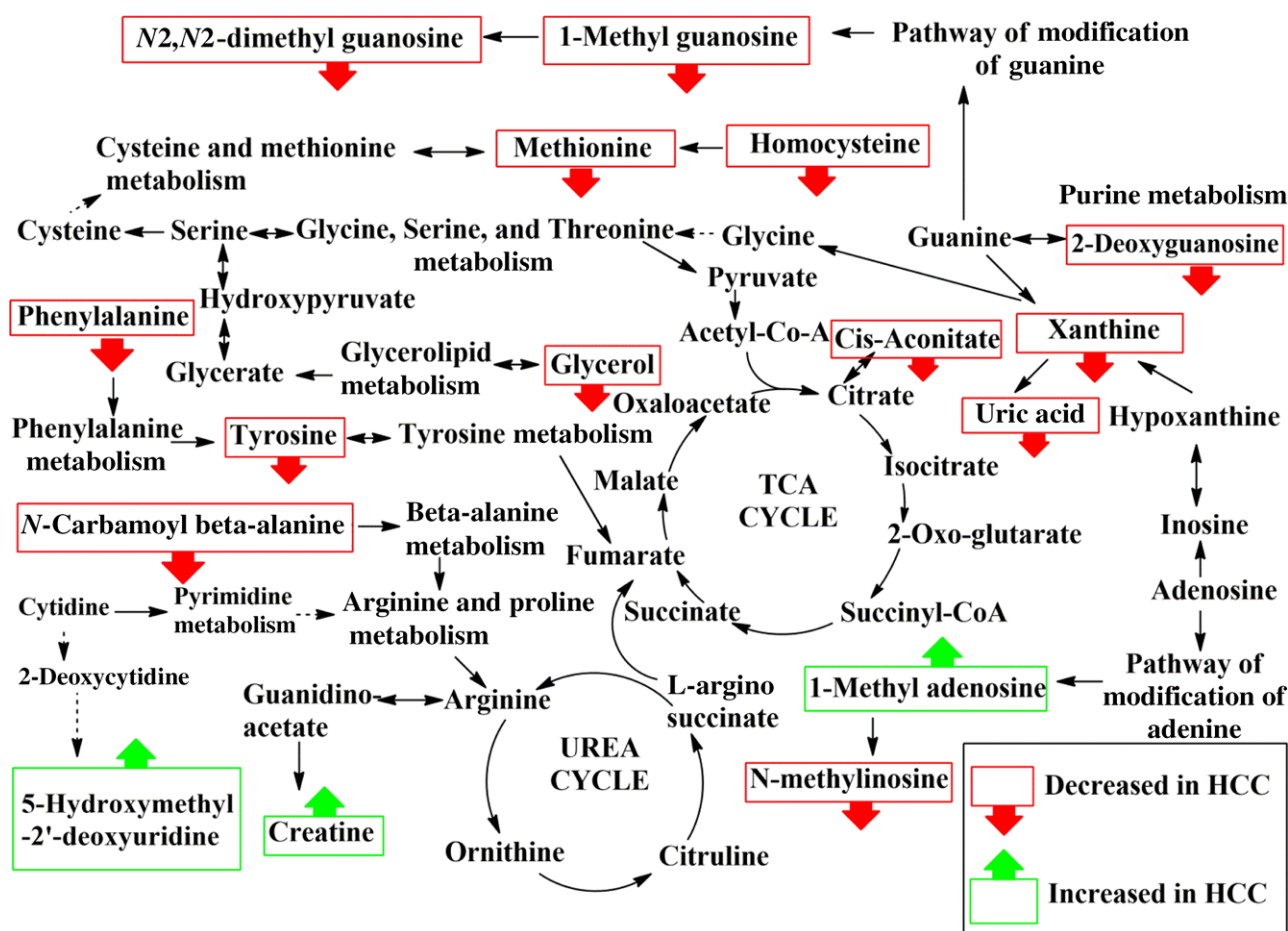
Figure 3. Depiction of metabolic pathways highlighting the metabolites that are altered in HCC.

Table 3. Molecular class assignments for the 73 metabolites detected by LC-MS/MS

Class[a]	Number	Percentage
Amino acids	26	36
Organic acids	22	30
Nucleosides and nucleotides	9	12
Purines and its derivatives	5	7
Amino ketones	3	4
Others	8	11

a) Reference: http://www.hmdb.ca.

has also been reported previously [3]. We also found that the mean level of xanthine decreased in HCC compared to HCV. Xanthine is formed from hypoxanthine by xanthine oxidase [36]. The activity of xanthine oxidase was observed to decrease in individuals with cancer [37]. Therefore, a decrease in the mean level of xanthine in HCC compared to HCV may be related to a decrease in xanthine oxidase activity.

Of the four metabolites with low *p*-values that were used for building the classification model, three metabo-

lites (methionine, *N*2,*N*2-dimethylguanosine, uric acid) were downregulated in HCC, while one (5-hydroxymethyl-2′-deoxyuridine) was elevated in HCC compared to HCV. Association of these metabolites with the metabolic pathways is highlighted in Fig. 3. The upregulated metabolite, 5-hydroxymethyl-2′-deoxyuridine, is reported to be associated with DNA repair and is thought to be involved in the pathogenesis of many diseases including cancer. A number of studies have reported that cancer patients often have higher levels of oxidative DNA damage as indicated by increased levels of 5-hydroxymethyl-2-deoxyuridine [38, 39].

The PLS-DA classification model developed using a panel of four highly significant metabolites, based on lowest *p*-value, provided high performance in terms of sensitivity (97%), specificity (95%), and AUROC curve (0.98%) and the results were better than those obtained based on metabolite selected using highest VIP scores (Fig. 2 and Supporting Information Fig. 2). As a comparison, a similar PLS-DA model developed using the three significant metabolites (creatinine, choline, and valine) obtained using NMR spectroscopy provided a sensitivity of 80%, specificity of 71%, and an area under the receiver-operating curve of 0.83 [27]. These results indicate

the potential of profiling a larger number of metabolites to distinguish HCC and HCV. The three metabolites identified by NMR were not considered for inclusion in the present PLS-DA model since, in the present study, creatinine was not targeted in the LC-MS/MS analysis, and choline and valine did not show significant differences in their levels. The NMR signal for choline also contains a contribution from phosphocholine that was not targeted in the LC-MS/MS analysis; valine can overlap with guanidinoacetate [30] and therefore make its accurate measurement challenging. Additional work on a larger set of samples is planned to validate the current and prior findings.

To conclude, this study reports the relative quantitative measurement of 73 targeted serum metabolites associated with many important metabolic pathways to profile patients with HCC and HCV by LC-MS/MS. Sixteen metabolites showed significantly altered levels between the two patient classes, while the top four biomarker candidates could be combined using multivariate statistical data analysis to provide an accurate model. In particular, the model distinguished the two patient groups with a sensitivity of 97%, specificity of 95%, and an AUROC of 0.98. These results are promising for identifying patients with underlying HCV who have developed HCC, and provide further insights into the altered metabolic processes that occur in the development of HCC in a high-risk patient population.

The authors have declared no conflict of interest.

5 References

[1] Lavanchy, D., *Clin. Microbiol. Infect.* 2011, *17*, 107–115.

[2] Anthony, P. P., *Histopathology* 2001, *39*, 109–118.

[3] Chen, T., Xie, G., Wang, X., Fan, J., Qiu, Y., Zheng, X., Qi, X., Cao, Y., Su, M., Wang, X., Xu, L. X., Yen, Y., Liu, P., Jia, W., Mol. Cell Proteom. 2011, *10*, M110.004945.

[4] Shariff, M. I. F., Gomaa, A. I., Cox, I. J., Patel, M., Williams, H. R. T., Crossey, M. M. E., Thillainayagam, A. V., Thomas, H. C., Waked, I., Khan, S. A., Taylor-Robinson, S. D., *J. Proteome Res.* 2011, *10*, 1828–1836.

[5] El-Serag, H. B., *Hepatology* 2002, *36*, S74–S83.

[6] Maasoumy, B., Wedemeyer, H., *Best Pract. Res. Clin. Gastroenterol.* 2012, *26*, 401–412.

[7] El-Serag, H. B., Davila, J. A., Petersen, N. J., McGlynn, K. A., *Ann. Intern. Med.* 2003, *139*, 817–823.

[8] Altekruse, S. F., McGlynn, K. A., Reichman, M. E., *J. Clin. Oncol.* 2009, *27*, 1485–1491.

[9] Siegel, R., Naishadham, D., Jemal, A., *CA Cancer J. Clin.* 2013, *63*, 11–30.

[10] Gao, H., Lu, Q., Liu, X., Cong, H., Zhao, L., Wang, H., Lin, D., *Cancer Sci.* 2009, *100*, 782–785.

[11] Zhang, J., Liu, L., Wei, S., Nagana Gowda, G. A., Hammoud, Z., Kesler, K. A., Raftery, D., *J. Thorac. Cardiovasc. Surg.* 2011, *141*, 469–475.

[12] Mayr, M., *Circ. Cardiovasc. Genet.* 2008, *1*, 58–65.

[13] Gowda, G. A., Zhang, S., Gu, H., Asiago, V., Shanaiah, N., Raftery, D., *Expert Rev. Mol. Diagn.* 2008, *8*, 617–633.

[14] Li, S., Liu, H., Jin, Y., Lin, S., Cai, Z., Jiang, Y., *J. Chromatogr. B Analyt. Technol. Biomed. Life Sci.* 2011, *879*, 2369–2375.

[15] Tan, Y., Yin, P., Tang, L., Xing, W., Huang, Q., Cao, D., Zhao, X., Wang, W., Lu, X., Xu, Z., Wang, H., Xu, G., *Mol. Cell. Proteomics* 2012, *11*, M111.010694.

[16] Wang, J., Zhang, S., Li, Z., Yang, J., Huang, C., Liang, R., Liu, Z., Zhou, R., *Tumour Biol.* 2011, *32*, 223–231.

[17] Zhou, L., Wang, Q., Yin, P., Xing, W., Wu, Z., Chen, S., Lu, X., Zhang, Y., Lin, X., Xu, G., *Anal. Bioanal. Chem.* 2012, *403*, 203–213.

[18] Patterson, A. D., Maurhofer, O., Beyoglu, D., Lanz, C., Krausz, K. W., Pabst, T., Gonzalez, F. J., Dufour, J. F., Idle, J. R., *Cancer Res.* 2011, *71*, 6590–6600.

[19] Chen, F., Xue, J., Zhou, L., Wu, S., Chen, Z., *Anal. Bioanal. Chem.* 2011, *401*, 1899–1904.

[20] Yin, P., Wan, D., Zhao, C., Chen, J., Zhao, X., Wang, W., Lu, X., Yang, S., Gu, J., Xu, G., *Mol. Biosyst.* 2009, *5*, 868–876.

[21] Wu, H., Xue, R., Dong, L., Liu, T., Deng, C., Zeng, H., Shen, X., *Anal. Chim. Acta* 2009, *648*, 98–104.

[22] Lin, X., Zhang, Y., Ye, G., Li, X., Yin, P., Ruan, Q., Xu, G., *J. Sep. Sci.* 2011, *34*, 3029–3036.

[23] Yang, J., Xu, G., Zheng, Y., Kong, H., Pang, T., Lv, S., Yang, Q., *J. Chromatogr. B* 2004, *813*, 59–65.

[24] Xue, R., Lin, Z., Deng, C., Dong, L., Liu, T., Wang, J., Shen, X., *Rapid Commun. Mass Spectrom.* 2008, *22*, 3061–3068.

[25] Wang, B., Chen, D., Chen, Y., Hu, Z., Cao, M., Xie, Q., Chen, Y., Xu, J., Zheng, S., Li, L., *J. Proteome Res.* 2012, *11*, 1217–1227.

[26] Patterson, A. D., Maurhofer, O., Beyoglu, D., Lanz, C., Krausz, K. W., Pabst, T., Gonzalez, F. J., Dufour, J. F., Idle, J. R., *Cancer Res.* 2011, *71*, 6590–6600.

[27] Wei, S., Suryani, Y., Gowda, G. A. N., Skill, N., Maluccio, M., Raftery, D., *Metabolites* 2012, *2*, 701–716.

[28] Bajad, S. U., Lu, W., Kimball, E. H., Yuan, J., Peterson, C., Rabinowitz, J. D., *J. Chromatogr. A* 2006, *1125*, 76–88.

[29] Lewis, G. D., Wei, R., Liu, E., Yang, E., Shi, X., Martinovic, M., Farrell, L., Asnani, A., Cyrille, M., Ramanathan, A., Shaham, O., Berriz, G., Lowry, P. A., Palacios, I. F., Tasan, M., Roth, F. P., Min, J., Baumgartner, C., Keshishian, H., Addona, T., Mootha, V. K., Rosenzweig, A., Carr, S. A., Fifer, M. A., Sabatine, M. S., Gerszten, R. E., *J. Clin. Invest.* 2008, *118*, 3503–3512.

[30] Wei, R., Li, G., Seymour, A. B., *Anal. Chem.* 2010, *82*, 5527–5533.

[31] Djukovic, D., Baniasadi, H. R., Kc, R., Hammoud, Z., Raftery, D., *Rapid Commun. Mass. Spectrom.* 2010, *24*, 3057–3062.

[32] Lai, H. S., Lee, J. C., Lee, P. H., Wang, S. T., Chen, W. J., *Semin. Cancer Biol.* 2005, *15*, 267–276.

[33] Asiago, V. M., Alvarado, L. Z., Shanaiah, N., Gowda, G. A., Owusu-Sarfo, K., Ballas, R. A., Raftery, D., *Cancer Res.* 2010, *70*, 8309–8318.

[34] Rocha, C. M., Barros, A. S., Gil, A. M., Goodfellow, B. J., Humpfer, E., Spraul, M., Carreira, I. M., Melo, J. B., Bernardo, J., Gomes, A., Sousa, V., Carvalho, L., Duarte, I. F., *J. Proteome Res.* 2010, *9*, 319–332.

[35] Yokota, H., Guo, J., Matoba, M., Higashi, K., Tonami, H., Nagao, Y., *J. Magn. Reson. Imaging* 2007, *25*, 992–999.

[36] Newaz, M. A., Adeeb, N. N. N., Muslim, N., Razak, T. A., Htut, N. N., *Clin. Exp. Hypertens* 1996, *18*, 1035–1050.

[37] Weber, G., *Clin. Biochem.* 1983, *16*, 57–63.

[38] Djuric, Z., Heilbrun, L. K., Simon, M. S., Smith, D., Luongo, D. A., LoRusso, P. M., Martino, S., *Cancer* 1996, *77*, 691–696.

[39] Evans, M. D., Saparbaev, M., Cooke, M. S., *Mutagenesis* 2010, *25*, 433–442.